Direct vaporization of an organic fluid in a parabolic trough solar collector

Simone Dugaria[1], Matteo Bortolato[1] and Davide Del Col[1]

[1] Department of Industrial Engineering (DII), University of Padova, Padova, Italy

Abstract

An innovative solar receiver for linear concentrating collectors is used for the direct vaporization of a low GWP halogenated fluid. Experiments have been conducted to determine the thermal performance of the collector during vaporization of an organic fluid that can be adopted for ORC cycle. The mass flow rate and the subcooling of the halogenated fluid entering the receiver have been varied, along with the outlet vapor quality and saturation pressure. The results of the experimental campaign reveal that the solar collector is able to vaporize this halogenated fluid at 85°C with 73% efficiency. A numerical model of the collector has been developed and validated against the experimental data. The estimated thermal performance of the collector is in good agreement with the experimental tests. The mean relative error in the prediction of the thermal efficiency of the collector results within 2%.

Key-words: HCFO-1233zd(E); solar direct vaporization; parabolic trough collector

Nomenclature

Symbols

A_a	Aperture area, m^2
c_{II}	Specific heat of the secondary fluid, J K^{-1} kg^{-1}
DNI	Direct Normal Irradiance, W m^{-2}
h	Specific enthalpy, J kg^{-1}
h_L	Specific enthalpy of the saturated liquid, J kg^{-1}
h_{LV}	Latent heat of vaporization, J kg^{-1}
$\dot{m}$	Mass flow rate, kg s^{-1}
p	Pressure, Pa
q	Heat flow rate, W
T	Temperature, °C
T_m^*	Reduced mean temperature, K m^2 W^{-1}
x	Vapor quality, -

Greek symbols

$\alpha_{r,coat}$	Absorbance of the coating layer, -
ρ_c	Reflectance of the collector's mirror, -
γ_r	Receiver intercept factor, -
η_{col}	Collector thermal efficiency, -

Subscripts

I	Primary fluid (HCFO-12333zd(E))
II	Secondary fluid (Cooling water)
HE	Heat Exchanger
in	Inlet
R	Receiver
out	Outlet

1. Introduction

Organic Rankine Cycle (ORC), unlike the traditional steam Rankine cycle, can work with low temperature heat sources, by using an organic fluid instead of water as working fluid (Peris et al., 2015). The selection of the organic working fluid (OWF) is a crucial choice in determining the performance and the cost of the system (Chen et al., 2010). For ORC systems coupled to low-grade heat sources, HFC-245fa has been considered by many authors the best choice (Cataldo et al., 2014, Quoilin et al., 2011). This is a common working fluid used in commercial ORCs generating mechanical power from low-temperature heat sources and for high-temperature heat pumps. Despite the excellent thermodynamic performance of HFC-245fa for the exploitation of low-grade heat source the growing sensitivity of the society on environmental issues will increasingly limit its use due to its high GWP (1030 according to Molés et al., 2015). Moles et al (2014) identified the halogenated fluid HCFO-1233zd(E) as valuable candidate for the future replacement of HFC-245fa in various applications. Despite the presence of the chlorine in its molecule, it presents an extremely small value (0.00034) of ODP (Patten and Wuebbles, 2010), due to its very short atmospheric lifetime. Its GWP value was recently reported to be lower than one (Myhre et al., 2014).

Besides the theoretical studies (Giuffrida, 2014, Heberle et al., 2016, Molés et al., 2014), very few experiments on the use of HCFO-1233zd(E) as HFC-245fa drop-in replacement for ORC have been presented in the literature. Eyerer et al. (2016) studied the applicability of HCFO-1233zd(E) as substitute for HFC-245fa in ORC system supplied by a heat source at 120 °C by comparing cycle efficiency and power output. The authors concluded that HCFO-1233zd(E) can be successfully used to replace HFC-245fa without major modifications in the system. It was found that the use of HCFO-1233zd(E) can lead to an increase of 6.92% in the thermal efficiency with

Selection and/or peer review under responsibility of Scientific Committee
doi:10.18086/swc.2017.17.01 Available at http://proceedings.ises.org

constant condensation and evaporation temperatures and constant isoentropic expansion efficiency. However, the net electric power generated by the ORC was 12.17% lower due to the largest volumetric flow rates of the HCFO-1233zd(E) required for the use of the system designed for HFC-245fa. In the work of Molés et al. (2016), an experimental evaluation of the working fluid HCFO-1233zd(E) as HFC-245fa replacement in ORC systems for low-temperature heat sources at different operating conditions has been conducted. Thermal and electrical powers resulted lower for HCFO-1233zd(E) than those for HFC-245fa at the same volumetric flow rate, due to the fact that the different densities of the working fluids. However, the net electrical efficiency was similar for both working fluids, ranging from 5% to 10%.

The exploitation of solar radiation can significantly contribute to reduce the consumption of conventional (non-renewable) energy sources and relieving associated environmental problems. A solar thermal system can be combined with ORC system according to two configurations: coupling with direct vaporization of the OWF or by using an intermediate solar circuit to heat a heat transfer fluid and evaporate the OWF in a separate heat exchanger. In a solar powered ORC system with direct vaporization of the OWF, the solar receiver coincides with the evaporator. By adopting this configuration is possible to simplify the system layout as the intermediate loop for transferring the heat from the solar collector to the OWF is no longer needed. It is expected that the direct vaporization of the OWF in the solar receiver allows to convert the solar energy collected by the solar system into the thermal energy of the OWF with a higher efficiency. In fact, this process takes place without the irreversibility associated with the heat transfer occurring in the heat exchanger/evaporator of the indirect vaporization. This aspect is particularly important in ORC systems where the temperature differences between the heat source and environment are quite low (around 100 °C).

Although, the feasibility of conventional steam Rankine cycles with direct vaporization of water in parabolic trough collectors (PTCs) has been extensively demonstrated (Eck et al., 2003, 2007), it has not yet been proved with organic fluids. This paper presents the experimental and numerical results on the direct vaporization of the halogenated fluid HCFO-1233zd(E) in an innovative aluminum flat absorber for medium temperature linear concentrating solar collectors.

2. Experimental apparatus and campaign

The small parabolic trough concentrator considered in this work is asymmetrical since the reflective optics extends from the vertex line to the mirror rim (Figure 1). This concentrator has been installed at the Solar Energy Conversion Lab of the Industrial Engineering Department, University of Padova (45.416°N, 11.883°E). The present concentrator exhibits an aperture width of 2.9 m, a rim angle of 78°, a focal length of 1.81 m and a trough length of 2.4 m, resulting in an aperture area slightly lower than 7 m^2. The reflecting optical system is made up by four back silvered glass facets arranged in two rows, which have a nominal reflectance of 96%, as provided by the manufacturer. Due to the small dimensions of the prototype, it is equipped with a two-axes solar tracking system to have the beam radiation normal to the aperture area without any cosine loss. The motion is governed by a solar algorithm when approaching the sun and by a sun sensor to achieve the best alignment.

Figure 1. Asymmetrical parabolic trough linear solar concentrator installed in the Solar Energy Conversion Lab of the University of Padova.

Figure 2. Bar-and-plate flat receiver arranged on the support bar of the collector under concentrated solar radiation during a test run.

The particular geometry of the parabolic trough concentrator is suitable to be coupled with a receiver provided with a flat geometry absorber. The innovative receiver considered in this work has been manufactured with bar-and-plate technology and is provided with an internal offset strip turbulator (Bortolato et al., 2016). The combined use of a high thermal conductivity material and a passive heat transfer enhancement technique in the absorber is a promising solution for linear concentrating devices. In order to minimize the incidence angle of the concentrated beams on the flat receiver, the optimal concentration plane of this system is 45° tilted with respect to the plane containing the focal line and the normal to the aperture area. The receiver presents a length equal to 1.2 m, which corresponds to half of the total trough length, and a width of 70 mm, thus, the resulting geometrical concentration ratio of the concentrating collector is equal to 42 (Figure 2).

2.1 Test facility

The test facility has been designed in order to measure the thermal efficiency of the solar concentrating collector during the vaporization of the fluid. A primary loop, where the halogenated fluid flows, is arranged on board the concentrating collector (Figure 3). The heat provided by the concentrated solar irradiance is dissipated through a heat exchanger to a secondary loop with cooling water. Both the loops are thermally insulated to limit heat losses towards the surroundings. The laboratory is equipped with a measuring system of the solar irradiance including a first class pyrheliometer mounted on a high precision solar tracker that is used to measure the direct normal irradiance (DNI). An anemometer measures the wind speed on the horizontal plane and the ambient air temperature is gauged by a Pt100 resistance temperature detector (RTD).

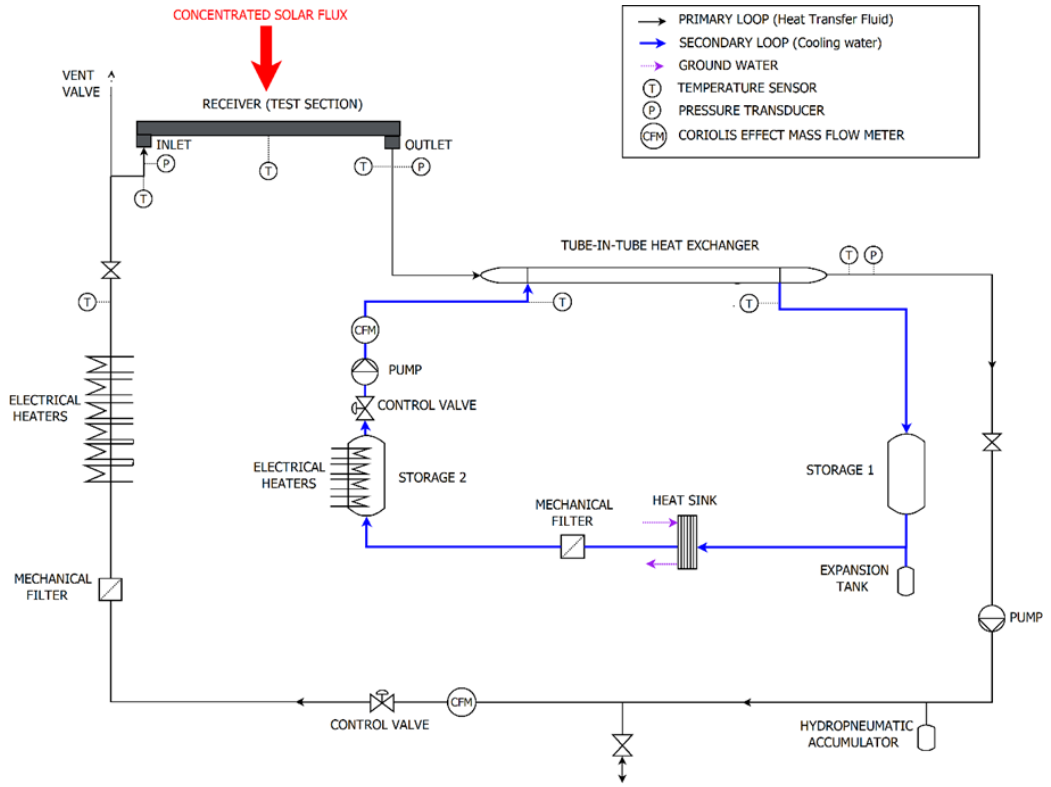

Figure 3. Sketch of the experimental test rig.

In the primary loop, after exiting the receiver, the heat transfer fluid (HCFO-1233zd(E)) enters a tube-in-tube heat exchanger, where the HCFO-1233zd(E) flows inside the inner tube, while the coolant (water) flows in the annulus. The pressure of the primary loop is regulated by a hydropneumatic accumulator with a fluoroelastomer diaphragm: this device plays an important role in direct vaporization tests as the working pressure determines the temperature of the generated vapor. Before entering the receiver, the halogenated fluid passes through a pre-heating section which consists of a electrical heater connected to a solid-state relay which is governed by a PID temperature controller. Temperatures and pressures of the organic fluid at inlet and outlet of the receiver and downstream of are measured by Pt100 RTDs and high precision absolute pressure transducers. Since the presence of a turbulator may penalize the hydraulic performance, accurate measurements of pressure drop have also to be carried out. In the

secondary loop, the controls on the cooling water mass flowrate and inlet temperature are useful to achieve constant conditions of the primary working fluid at the inlet of the receiver. The temperatures of the water at the inlet and at the outlet of the tube-in-tube heat exchanger are measured by Pt100 RTDs. All the measured quantities are recorded by a data logger with sampling rate of 3 s and the collected data are reduced in a MATLAB environment by calculating the fluid properties with NIST Refprop Version 9.0 (Lemmon et al., 2010).

2.2 Experimental technique and data reduction

The test methods to determine the thermal performance of solar concentrating collectors, namely the steady state method in the ASHRAE 93:2010 standard and the quasi dynamic method in EN ISO 8609:2013 standard, refer only to liquid or air heating devices. This means that the useful heat gained by the working fluid can be calculated considering its temperature increase inside the solar collector. There are no standard procedures to experimentally define the thermal efficiency of a solar concentrating collector performing direct steam generation, when a latent heat transfer is involved. The procedure proposed by Bortolato et al. (2016), has been adopted to evaluate the thermal performance of the concentrating solar collector during the vaporization of the halogenated fluid. During the test runs, the organic fluid enters the test section as subcooled liquid and its thermodynamic condition is completely determined by the temperature and pressure measurements at the inlet of the receiver. The fluid exits the receiver as saturated vapor and then it is condensed and subcooled in the tube-in-tube heat exchanger. The thermodynamic state of the halogenated fluid at the outlet of the receiver under saturated conditions can be experimentally defined by applying the energy balance to the heat exchanger, under the reasonable hypothesis of negligible heat losses towards the surroundings. The saturation temperature is assumed equal to the temperature measured at the outlet of the receiver because, during the two-phase test runs, the pressure drop across the receiver is very small.The specific enthalpy $h_{out,R,I}$ and of vapor quality $x_{out,R,I}$ of the saturated steam at the outlet of the receiver can be expressed as reported in the following expressions

$$h_{out,R,I} = h_{out,HE,I}\left(T_{out,HE,I}, p_{out,HE,I}\right) + \frac{\dot{m}_{II}\, c_{II}\left(T_{out,HE,II} - T_{in,HE,II}\right)}{\dot{m}_I} \qquad (2.1)$$

$$x_{out,R,I} = \frac{h_{out,R,I} - h_L\left(T_{out,R,I}\right)}{h_{LV}\left(T_{out,R,I}\right)} \qquad (2.2)$$

The experimental results are presented in a diagram plotting the experimental thermal efficiency η_{col}, as a function of the reduced mean temperature T_m^* along with the obtained efficiency curve of the collector.

$$\eta_{col} = \frac{q_I}{\mathrm{DNI}\, A_{ap}} = \frac{\dot{m}_I \left(h_{out\,R,I} - h_{in\,R,I}\right)}{\mathrm{DNI}\, A_{ap}} \qquad (2.3)$$

$$T_m^* = \frac{\frac{\left(T_{out\,R,I} + T_{in\,R,I}\right)}{2} - T_{amb}}{\mathrm{DNI}} = \frac{T_{m\,R,I} - T_{amb}}{\mathrm{DNI}} \qquad (2.4)$$

In order to express the reduced mean temperature under two-phase flow, it is required the introduction of the equivalent mean temperature of the fluid during direct vaporization of the fluid. Since the working fluid enters as subcooled liquid, both sensible and latent heat transfers occur inside the receiver of the solar concentrating collector. Hence, the equivalent mean temperature of the fluid shall be assumed as a weighted average temperature based on the enthalpy changes associated to the sensible and latent heat transfers (Equation 2.5).

$$T_{m\,eq,I} = \frac{\left(\frac{T_{out,R,I} + T_{in,R,I}}{2}\right)\left(h_L\left(T_{out,R,I}\right) - h_{in,R,I}\right) + T_{out,R,I}\left(h_{out,R,I} - h_L\left(T_{out,R,I}\right)\right)}{h_{out,R,I} - h_{in,R,I}} \qquad (2.5)$$

2.3 Experimental uncertainty analysis

Before the test campaign, the primary loop is evacuated and then filled with HCFO-1233zd(E). After a preconditioning period of 20 min, during each test sequence, that lasts for 3 hours minimum, the collected data are averaged every 10 min and the following criteria have been satisfied during tests:

- the inlet temperature of the subcooled liquid is kept stable within ±1 °C as compared to its mean value;
- the HCFO-1233zd(E) mass flow rate is kept stable within ±2% as compared to the mean value;
- the thermodynamic vapor quality at the outlet of the receiver must be higher than 0.1.

The uncertainty analysis has been performed in agreement with the guidelines provided by the “Guide to the

Expression of Uncertainty in Measurement" (International Organization for Standardization, 2008). Type B uncertainties of the measured parameters are reported in Table 1 with a level of confidence of 95%.

Table 1. Type B uncertainty of measured parameters during direct vaporization in bar-and-plate flat receiver under concentrated solar radiation.

Ambient air temperature	± 0.07°C
Fluid temperature in primary and secondary loops	± 0.035°C
Coriolis effect mass flow meters	± 0.3 kg h^{-1} (cooling water) ± 0.07 kg h^{-1} (HCFO-1233zd(E))
Pressure of the fluid in the primary loop	± 0.023 bar
Direct normal irradiance	± 3% of measured value
Wind speed	± (0.1 m/s + 1% of measured value)

With respect to the parameters which are not directly measured, their combined standard uncertainty can be calculated by applying the law of error propagation with level of confidence of 95%. Type A uncertainty is the standard deviation of the mean and, in the present tests, it comes out considering 200 readings collected over the averaging time period of 10 min.

2.4 Experimental results

The experimental tests have been carried out during the month of August 2016 at the average evaporation pressure of 7.5 bar corresponding to 85°C saturation temperature. During the tests, the ambient temperature was in the range 28 – 35°C and the values of the direct normal irradiance were between 700 W m^{-2} and 920 W m^{-2}. The mass flow rate of the halogenated fluid has been varied between 46 kg $h^{-1}$and 106 kg h^{-1}. The experimental results show that the collector thermal efficiency η_{col}, calculated according to Equation 2.3, was around 73%. Figure 4 reports the effects of the outlet vapor quality on the collector efficiency during the vaporization of the halogenated fluid Considering that the extended uncertainty of the collector efficiency is ±3%, it can be concluded that the outlet vapor quality has a negligible effect on the collector efficiency. This remarkable result suggest that it is possible to vaporize almost completely the halogenated fluid in the bar-and-plate receiver without any losses of efficiency. In Figure 5, where the thermal efficiency of the collector is plotted against the inlet subcooling, it can be noted that also the inlet subcooling did not significantly affect the efficiency of the solar collector.

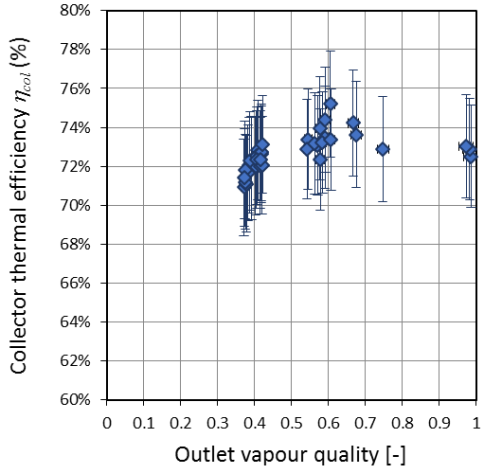

Figure 4. Experimental thermal efficiency of the solar collector as a function of the outlet vapor quality.

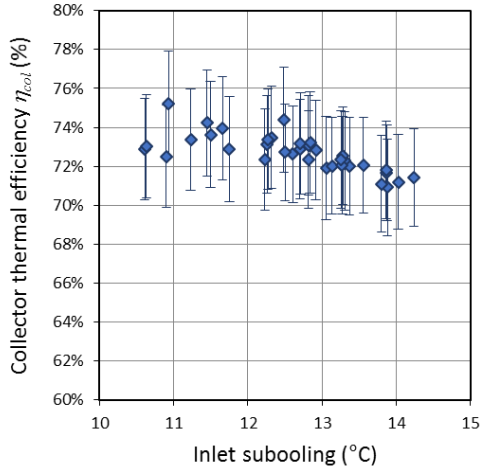

Figure 5. Experimental thermal efficiency of the solar collector as a function of the inlet subcooling.

Figure 6 reports the pressure drop through the bar-and-plate flat receiver as a function of the mass flow rate during the vaporization test runs of the halogenated fluid. This Figure provides only a general trend of the pressure drop, because the plotted values are lower than the experimental uncertainty of the pressure transducers. Anyway, the result shows that the designed absorber is capable of vaporize the fluid HCFO-1233zd(E) with a limited pressure drop, implying a low electrical consumption for the circulating pump.

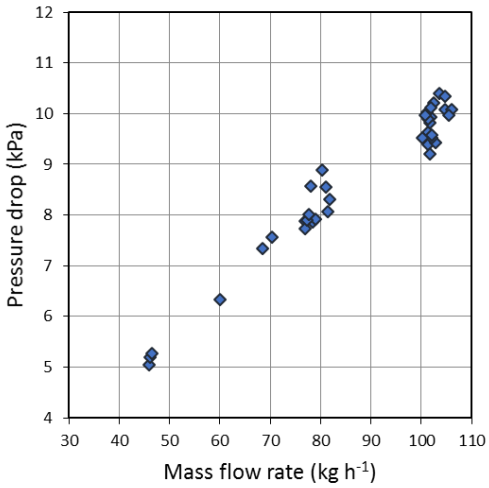

Figure 6. Pressure drop through the receiver as a function of the mass flow rate during vaporization.

3. Numerical model

A numerical model of the solar absorber system is developed in order to predict the performance of the receiver installed in a linear concentrating system. The receiver has been discretized along its length in several segments. Each segment constitutes a control volume where a zero-dimensional steady-state energy balance is applied. The zero-dimensional thermal resistance network is reported in Figure 7, where the external surfaces (front, back and lateral) of the absorber, the external surface of the insulation layer on the back of the receive, the internal surface of the absorber in contact with the fluid and the fluid itself constitute the thermal nodes of the model.

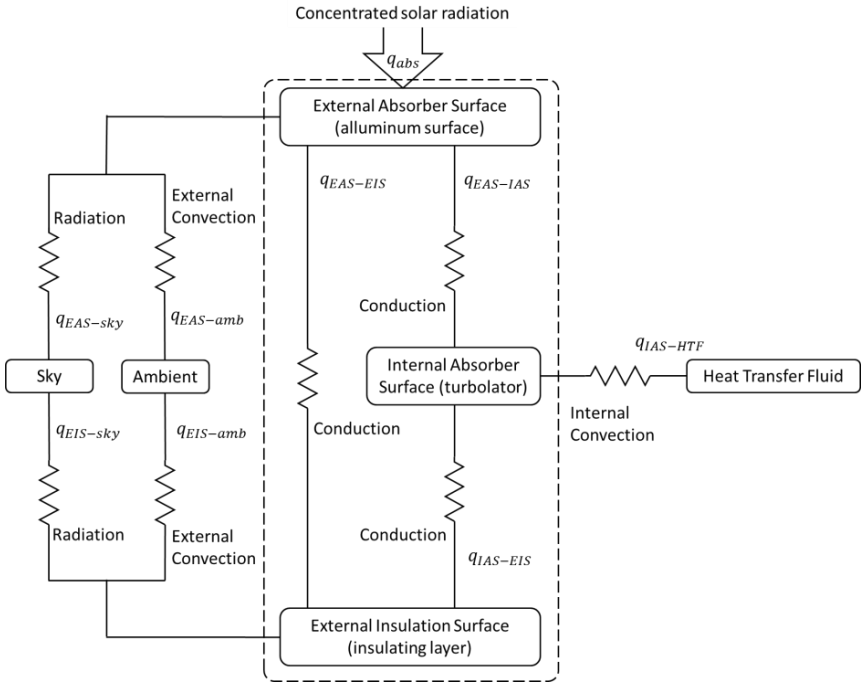

Figure 7. – Thermal resistance network representing the dimensionless model of the bar-and-plate flat receiver.

In the model, the effective incident concentrated solar radiation, net to the losses in the optical concentration, is mainly absorbed by the surface coating of the absorber and the absorbed heat flow rate q_{abs} has been considered as:

$$q_{abs} = DNI\ A_a \alpha_{r,coat} (\rho_c \gamma_r) \qquad (3.1)$$

Some energy absorbed into the coating is conducted through the absorber and transferred to the fluid $q_{EAS\text{-}HTF}$ by convection or by vaporization, while the rest is conducted through the insulating layer to the back surface $q_{EAS\text{-}EIS}$.

The remaining energy is lost directly to the environment by convection and radiation ($q_{EAS\text{-}amb}$, $q_{EIS\text{-}amb}$, $q_{EAS\text{-}sky}$, $q_{EIS\text{-}sky}$). The model assumes that all temperatures, heat flow rates and thermodynamic properties are uniform around the perimeter of the receiver. With reference to Figure 7, the energy balance equations are determined by conserving energy at each surface of the receiver cross-section:

$$q_{abs} = q_{EAS-amb} + q_{EAS-sky} + q_{EAS-IS} + q_{EAS-EBS} \quad (3.2)$$

$$q_{IAS-HTF} = q_{EAS-IS} - q_{IS-EIS} \quad (3.3)$$

$$q_{EAS-EIS} + q_{IAS-EIS} = q_{EBS-amb} + q_{EIS-sky} \quad (3.3)$$

Correlations for heat transfer in single- and two-phase flows are implemented in the energy balances depending on the flow conditions in each control volume. Convective losses from the outer surface of the absorber have been modelled considering a forced convection mechanism in which the wind speed plays the main role. Radiative heat losses to the environment depend on the difference between the temperature of the external surface of the receiver and the apparent temperature of the sky assumed 8 °C below the ambient air temperature (Forristall, 2003).

The heat transfer from the external to the internal (turbulator) surface of the absorber can be treated as heat conduction in a rectangular cross section hollow body with the inner and outer surfaces at constant temperatures. In the considered receiver, given the high conductivity of the aluminum, which the absorber is made, it is reasonable to assume that the internal surface temperature is fairly constant.

Finally, to calculate the heat flow rate gained by the heat transfer fluid in the absorber, two heat transfer mechanism have been considered. Convective liquid heating occurs when the fluid is subcooled or saturated liquid and the wall temperature of the inner surface is lower than the saturation temperature, while a two-phase heat transfer occurs when the temperature of the internal surface in contact with the fluid is above its saturation temperature. To calculate the convective heat transfer coefficient when the liquid is heated, the procedure proposed by Manglik and Bergles (1995) is adopted. In the two-phase heat transfer, vaporization of the fluid can occur already in the presence of undercooled liquid. The formulation proposed by Liu and Winterton (1991) at the average vapor quality between inlet and outlet conditions of the control volume is applied to calculate the heat transfer coefficient between the inner wall and the vaporizing fluid.

The numerical model is implemented in Matlab® in a block diagram Simulink® environment. The thermophysical properties of the fluids are calculated with NIST Refprop Version 9.0 (Lemmon et al., 2010). The model includes the parameters used to describe the concentrator's optical performance (i.e. the nominal reflectance of the mirrors, optical properties of the external surface of the receiver), the geometric properties of the receiver and of its internal turbulator. The inputs of the model are the direct normal irradiance, the temperature and the velocity (wind speed) of the ambient air, the inlet temperature and mass flow rate of the heat transfer fluid in the receiver, assuming that it is always in conditions of subcooled liquid and its saturation pressure. The model estimates the temperatures at each of the considered thermal nodes in each receiver's segment as long as the convergence criteria based on the local and global thermal balances are not satisfied. Once the convergence is reached, the model provides the useful heat flow rate gained by the fluid, the average fluid temperature, the outlet temperature and vapor quality for each segment of the receiver, and finally, the thermal efficiency of the solar thermal collector.

3.1 Model validation

The results of the numerical simulations are compared against experimental data to assess the accuracy of the model. The difference between the estimated value of the collector efficiency and the collect data are plotted as function of the mass flow rate of the halogenated fluid. Figure 8 shows that the estimated thermal performance of the collector is in good agreement with that determined through the experimental tests. The prediction of the thermal efficiency displays a prediction error within 2%.

The validated numeric model has been used to perform an estimation of thermal performance of the collector including vaporization of the halogenated fluid up to a saturation temperature of 120 °C. The result of these simulations is shown in Figure 13. For these simulations, the values of the mass flow rate are assumed according to the inlet subcooling, so that the outlet vapor quality resulted between 0.55 and 0.6. This is done to prevent the onset of dryout phenomenon and the use of the Liu and Winterton (1991) outside its validity range. The ambient temperature is considered equal to 30 °C. From the numerical predictions, it results that it is possible to vaporize

the halogenated fluid HCFO-1233zd(E) inside the modelled receiver at a saturation temperature of 130 °C with a thermal efficiency of solar collector higher than 65%. Even though, the experimental efficiency curve plotted in Figure 9 is extended from its original range of definition, it results in very good accordance with the simulated efficiency curve.

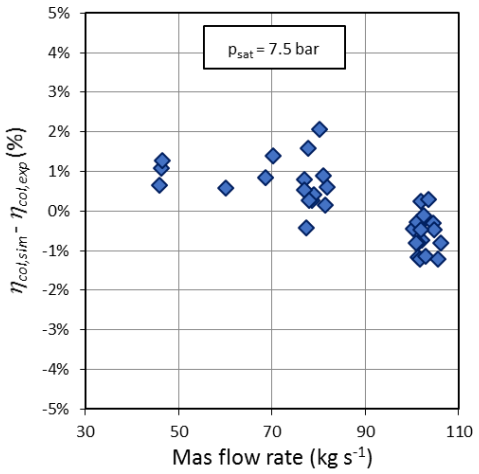

Figure 8 – Difference between simulated and measured values of the collector efficiency as a function mass flow rate.

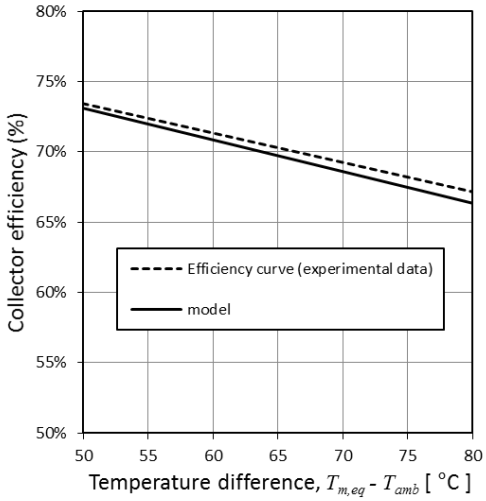

Figure 9. Simulated and experimental efficiency curves as a function of the temperature difference between the calculated mean condition of the fluid and the ambient.

4. Conclusions

An innovative solar receiver for linear concentrating collectors has been experimentally tested for the direct vaporization of a low-GWP halogenated fluid. The conducted experiments allow to determine the thermal performance of the collector composed by a parabolic trough concentrator and the flat solar receiver. During the tests the mass flow rate and the subcooling of the halogenated fluid entering the receiver have been varied to obtain different values of the outlet vapor quality.

The results of the experimental campaign reveal that the solar collector is able to vaporize the HCFO-1233zd(E) at 7.5 bar saturation and outlet vapor quality between 0.37 and 0.98 with a mean efficiency of 73%. In the present operating conditions, the mass flow rate and the subcooling of the halogenated fluid entering the receiver display a negligible influence on the performance of the collector.

A numerical model of the receiver has been developed in Matlab®. This model divides the receiver in several segments and is capable to estimate the temperatures at each thermal node in each receiver's segment providing the heat flow rate gained by the fluid, the average fluid temperature, the outlet temperature and vapor quality at each segment of the receiver, and finally, the thermal efficiency of the solar thermal collector. The results of the numerical simulations were compared against experimental data to validate the model. The estimated thermal performance of the collector is in good agreement with the experimental tests. The prediction of the thermal efficiency of the collector displays error within 2%. The model can be used to perform an estimation of thermal performance of the collector with vaporization of the halogenated fluid up to 120°C saturation temperature. It results that it is possible to vaporize the halogenated fluid HCFO-1233zd(E) at an outlet vapor quality between 0.55 and 0.6 with a thermal efficiency of the solar collector higher than 65%.

5. References

Bortolato, M., Dugaria, S., Del Col, D., 2016. Experimental study of a parabolic trough solar collector with flat bar-and-plate absorber during direct steam generation. Energy 116, Part 1, 1039-1050.

Cataldo, F., Mastrullo, R., Mauro, A.W., Vanoli, G.P., 2014. Fluid selection of Organic Rankine Cycle for low-temperature waste heat recovery based on thermal optimization. Energy 72, 159-167.

Chen, H., Goswami, D.Y., Stefanakos, E.K., 2010. A review of thermodynamic cycles and working fluids for the conversion of low-grade heat. Renewable and Sustainable Energy Reviews 14, 3059-3067.

Eck, M., Uhlig, R., Mertins, M., Häberle, A., Lerchenmüller, H., 2007. Thermal load of direct steam-generating absorber tubes with large diameter in horizontal linear fresnel collectors. Heat transfer engineering 28, 42-48.

Eck, M., Zarza, E., Eickhoff, M., Rheinländer, J., Valenzuela, L., 2003. Applied research concerning the direct steam generation in parabolic troughs. Solar Energy 74, 341-351.

Eyerer, S., Wieland, C., Vandersickel, A., Spliethoff, H., 2016. Experimental study of an ORC (Organic Rankine Cycle) and analysis of R1233zd-E as a drop-in replacement for R245fa for low temperature heat utilization. Energy 103, 660-671.

Forristall, R., 2003. Heat Transfer Analysis and Modeling of a Parabolic Trough Solar Receiver Implemented in Engineering Equation Solver.

Giuffrida, A., 2014. Modelling the performance of a scroll expander for small organic Rankine cycles when changing the working fluid. Applied Thermal Engineering 70, 1040.

Heberle, F., Schifflechner, C., Brüggemann, D., 2016. Life cycle assessment of Organic Rankine Cycles for geothermal power generation considering low-GWP working fluids. Geothermics 64, 392-400.

International Organization for Standardization, 2008. ISO/IEC Guide 98-3:2008; Uncertainty of Measurement -- Part 3: Guide to the Expression of Uncertainty in Measurement (GUM:1995), Geneve, Switzerland.

Lemmon, E.W., Huber, M.L., McLinden, M.O., 2010. NIST Standard ReferenceDatabase 23: Reference Fluid Thermodynamic and Transport Properties - REFPROP. 9.0.

Liu, Z., Winterton, R.H.S., 1991. A general correlation for saturated and subcooled flow boiling in tubes and annuli, based on a nucleate pool boiling equation. International Journal of Heat and Mass Transfer 34, 2759-2766.

Manglik, R.M., Bergles, A.E., 1995. Heat transfer and pressure drop correlations for the rectangular offset strip fin compact heat exchanger. Experimental Thermal and Fluid Science 10, 171-180.

Molés, F., Navarro-Esbrí, J., Peris, B., Mota-Babiloni, A., 2016. Experimental evaluation of HCFO-1233zd-E as HFC-245fa replacement in an Organic Rankine Cycle system for low temperature heat sources. Applied Thermal Engineering 98, 954-961.

Molés, F., Navarro-Esbrí, J., Peris, B., Mota-Babiloni, A., Barragán-Cervera, Á, Kontomaris, K., 2014. Low GWP alternatives to HFC-245fa in Organic Rankine Cycles for low temperature heat recovery: HCFO-1233zd-E and HFO-1336mzz-Z. Applied Thermal Engineering 71, 204-212.

Molés, F., Navarro-Esbrí, J., Peris, B., Mota-Babiloni, A., Kontomaris, K., 2015. Thermodynamic analysis of a combined organic Rankine cycle and vapor compression cycle system activated with low temperature heat sources using low GWP fluids. Applied Thermal Engineering 87, 444-453.

Myhre, G., Shindell, D., Bréon, F.M., Collins, W., Fuglestvedt, J., Huang, J., et al., 2014. Chapter 8: anthropogenic and natural radiative forcing, in Stocker, D., Qin, G.-., Plattner, M., Tignor, S.K., Allen, J.B., et al. (Eds.), Climate Change 2013: The Physical Science Basis : Working Group I Contribution to the Fifth Assessment Report of the Intergovernmental Panel on Climate Change. Cambridge University Press, New York.

Patten, K.O., Wuebbles, D.J., 2010. Atmospheric lifetimes and Ozone Depletion Potentials of trans-1-chloro-3,3,3-trifluoropropylene and trans-1,2-dichloroethylene in a three-dimensional model. Atmospheric Chemistry and Physics 10, 10867-10874.

Peris, B., Navarro-Esbri, J., Moles, F., Gonzalez, Mota-Babiloni, A., 2015. Experimental characterization of an ORC (organic Rankine cycle) for power and CHP (combined heat and power) applications from low grade heat sources. Energy 82, 269-276.

Quoilin, S., Orosz, M., Hemond, H., Lemort, V., 2011. Performance and design optimization of a low-cost solar organic Rankine cycle for remote power generation. Solar Energy 85, 955-966.